Carrier spin polarization in digital Mn/GaAs ferromagnetic structures studied with hot electron photoluminescence

V. F. Sapega,[1,2,*] A. Trampert,[1] and K. H. Ploog[1]
[1]*Paul-Drude-Institut für Festkörperelektronik, Hausvogteiplatz 5-7, D-10117 Berlin, Germany*
[2]*Ioffe Physico-Technical Institute, Russian Academy of Sciences, 194021 St. Petersburg, Russia*
(Received 29 January 2008; published 2 June 2008)

The effect of ferromagnetic layers on the spin polarization of holes and electrons in digital Mn/GaAs ferromagnetic heterostructures (DFHs) is studied with hot electron photoluminescence. We show that carriers in the GaAs interlayers experience a strong exchange interaction with the ferromagnetic interfaces. This exchange field rapidly decreases with increasing distance between the ferromagnetic Mn δ layers. The relaxation of the ferromagnetic properties of the digital structures is caused by compensation of the holes mediating the ferromagnetism of DFHs by electrons originating from the GaAs interlayers. For comparison, the polarization of holes in granular MnAs:GaAs, which consists of MnAs nanocrystals embedded in a GaAs matrix, is also studied. In this case, the holes in the GaAs matrix do not experience any strong magnetic fields from the ferromagnetic MnAs nanocrystals.

DOI: 10.1103/PhysRevB.77.245301 PACS number(s): 78.30.Fs, 76.30.Pk, 75.50.Pp

I. INTRODUCTION

Since the discovery of ferromagnetism in III–V diluted magnetic semiconductors (DMSs) in 1996,[1] these materials and its nanostructures have attracted considerable interest because of the feasibility to integrate ferromagnetic properties into semiconductors. The main goal of research in the following decade was the increase of the Curie temperature (T_C), which is limited by now to about 170 K in ternary (Ga,Mn)As alloys.[2] The application of the delta doping technique in so-called Mn/GaAs digital ferromagnetic heterostructures (DFHs)[3] was believed to induce a higher Curie temperature due to the locally confined high Mn concentration. The control of the GaAs layer thickness separating the Mn δ layers should allow the control of the ferromagnetic properties (Curie temperature and coercive force) as well as the manipulation of the spin polarization of carriers in the GaAs interlayer regions. The expected higher Curie temperature has not yet been verified. Instead, it was found that the magnetic properties of the whole system strongly depend on the GaAs interlayer thickness[3–6] as well as on the local structure and effective chemical valency of Mn atoms in Mn/GaAs DFHs.[7] On the other hand, the carrier polarization in the ferromagnetic layers and in the interlayer regions has not been investigated so far. Of particular importance for applications of DMS in spintronic devices is the effect of the ferromagnetic layers on the spin polarization of carriers and vice versa.

Another means to locally increase the Mn content in the GaAs matrix up to the formation of ferromagnetic MnAs nanocrystals (cluster) to increase the Curie temperature has been demonstrated by Moreno *et al.*[8,9] by using rapid thermal annealing (RTA) of low temperature-grown ternary (Ga,Mn)As alloys. This approach should also open the possibility to manipulate the carrier spin polarization in the GaAs matrix. However, ferromagnetic binary MnAs is hexagonal and exhibits metallic behavior. The effect of these metallic ferromagnetic nanocrystals on the carrier polarization in the surrounding GaAs matrix is thus expected to be different in this so-called granular GaAs:MnAs material.

In the present paper, we have directly probed the carrier polarization in ferromagnetic Mn/GaAs DFHs by means of hot electron photoluminescence (HPL).[10,11] We demonstrate that an increase in the GaAs interlayer thickness softens the magnetic properties of the ferromagnetic layers as well as reduces the carrier polarization. The decrease in the hole polarization is explained by the in-plane stress induced by thick GaAs interlayers in between the Mn δ sheets. We studied the effect of rapid thermal annealing (RTA) on carrier polarization in nominally ferromagnetic ternary (Ga,Mn)As alloys. In contrast to Mn/GaAs DFHs, in the granular GaAs:MnAs formed during RTA, the spin polarization of the carriers in the GaAs matrix exhibits a clear paramagneticlike behavior. The ferromagnetic ordering that exists in the ternary (Ga,Mn)As starting material is hence destroyed by the phase separation induced by rapid thermal annealing.

II. SAMPLES AND EXPERIMENT

The Mn/GaAs DFH samples were grown on Si-doped GaAs(001) substrates by standard solid-source molecular beam epitaxy (for details, see Ref. 4). After deposition of a high-temperature GaAs buffer layer of 450 nm thickness at 580–600 °C, the substrate temperature was reduced to 250 °C and a LT-GaAs buffer layer was grown with a thickness of 5 nm, followed by the Mn/GaAs heterostructure that was grown by alternately opening the Ga and Mn shutters at a constant As_4 flux. Finally, a capping layer of LT-GaAs was deposited. During growth, the reflection high-energy electron diffraction (RHEED) patterns and the specular RHEED beam intensity were recorded as a function of time. In order to clarify the relationship between the RHEED features and the actual nanostructure of the samples, transmission electron microscopy (TEM) measurements were carried out. Detailed TEM studies were of particular importance for the evaluation of the structure of granular GaAs:MnAs materials. The Mn concentration in the experiments was calibrated by secondary ion mass spectroscopy (SIMS) carried out on cor-

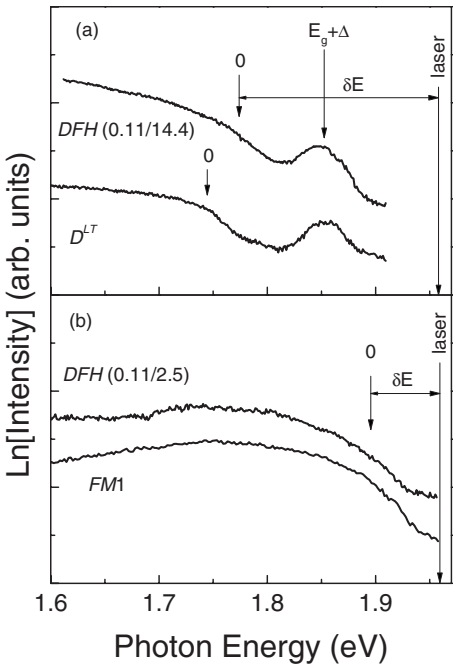

FIG. 1. HPL spectra of samples (a) bulk LT GaAs:Mn and DFH (0.11/14.4) (b) bulk DMS and DFH (0.11/2.5) excited with a He-Ne laser (1.96 eV) at $T=5$ K. The arrows labeled "0" indicate the energy for recombination of electrons from the point of generation. The PL band related to recombination of spin-orbit split holes with Mn double donors is labeled $E_G+\Delta$.

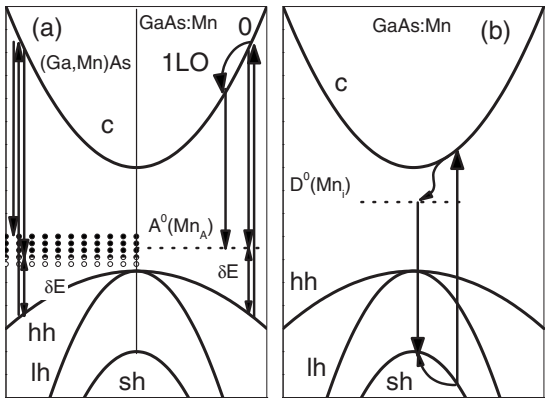

FIG. 2. (a) Schematic of HPL spectroscopy. The vertical arrows on the right and left show the excitation of the electrons from the heavy-hole valence band to the conduction band. The luminescence transitions from the point of creation and after emission of 1LO-phonons are indicated by the vertical arrows pointing down. The horizontal dashed line on the right presents monoenergetic distribution of the acceptor states in doping regime. The occupied (solid circles) and empty (open circles) impurity band states in the DMS case are shown on the left. The luminescence transitions of hot electrons to the upper and lower impurity band states of DMS are shown by vertical arrows pointing down. (b) The origin of the $E_G+\Delta$ band in GaAs:Mn. The vertical arrows pointing up and down show the excitation and recombination channels, respectively. The horizontal dashed line shows the interstitial Mn double-donor state.

responding reference samples. To distinguish the samples, we use the notation (A/B) nm, where A denotes the thickness of the Mn δ layer, while B denotes the thickness of the GaAs interlayers. It was demonstrated in accompanying studies that the maximum thickness of the Mn δ layer to preserve the structural integrity of the GaAs host lattice is 0.11 nm.[3,4,7] Therefore, in this work we have selected samples with a fixed Mn δ layer thickness of 0.11 nm and different GaAs interlayer thicknesses varying in the range of 2.5–14.4 nm and a fixed number of periods (40). One nominally ferromagnetic (Ga,Mn)As ternary alloy (sample FM2) with a Curie temperature of 35 K was subjected to the RTA treatment. The heating time from 200 to 700 °C was 20 s, and the cooling time to 400 °C was 12 s. This RTA-treated sample $FM2^{RTA}$ contains large hexagonal MnAs clusters, as revealed by detailed high-resolution x-ray diffraction and TEM measurements,[8] and it exhibits clear and strong ferromagnetic behavior. The Curie temperature for this sample was found to be ~330 K, which is even higher than the Curie temperature of bulk MnAs ($T_C=318$ K). In addition, a Mn-doped 1000 nm thick GaAs layer[11] (5×10^{17} cm^{-3}) grown at 560 °C and low temperature grown (250 °C) doped (5×10^{17} cm^{-3}) and ferromagnetic (Ga,Mn)As (with $x=0.043$)[11] were used as reference samples R1, D^{LT}, and FM1, respectively.

Superconducting quantum interference device (SQUID) magnetometry was used to determine the magnetic properties of the Mn/GaAs DFH's. The hot-electron photoluminescence (HPL) spectra were measured at $T=5$ K and in magnetic fields up to 10 T, in the backscattering Faraday geometry, by using the setup described in detail in Ref. 11. In the Faraday geometry, the circular polarization of the HPL was measured by utilizing a photoelastic modulator (PEM). The degree of circular polarization was defined by the common expression $\rho_c=(I^+-I^-)/(I^++I^-)$, where I^+ and I^- are the luminescence intensities with σ^+ and σ^- polarization, respectively.

III. RESULTS AND DISCUSSION

A. Hot electron photoluminescence polarization in digital ferromagnetic heterostructures

Figure 1 shows the HPL spectra obtained from two Mn/GaAs DFHs, a reference ternary (Ga,Mn)As alloy DMS (FM1), and a Mn-doped p-GaAs (D^{LT}) sample. The HPL spectra obtained from Mn-doped GaAs at low temperatures are due to the recombination of hot electrons with acceptor-bound holes (i.e., $1hh\rightarrow1e\rightarrow A^0$ type transitions), as schematically illustrated in Fig. 2. All of the DFH samples exhibit a higher-energy photoluminescence tail originating from radiative recombination of hot electrons with holes bound to single Mn acceptors or to the Mn acceptor impurity band. This assignment is based on the comparison of the spectra from the DFH samples to those obtained from the DMS (FM1) and the doped (D^{LT}) sample. A careful inspection of the spectra from the DFH, bulk DMS and doped samples clearly reveals that the spectral features of the DFH samples strongly depend on the thickness of the GaAs interlayers separating the ferromagnetic Mn δ layers. Indeed, the HPL spectrum obtained from the sample (0.11/2.5) nm with the smallest distance between the constituent ferromagnetic

layers is very similar to that observed in the DMS sample, while sample (0.11/7.2) nm evidences the similarity with the Mn-doped sample. We also observe a strong suppression (about 1 order of magnitude) of the HPL intensity when increasing the distance between the Mn δ layers.

To analyze the HPL spectra from Mn/GaAs DFHs, we have to take into account that both the δ doped and the undoped interlayer regions contribute to the observed HPL. Indeed, the DFH structures contain heavily Mn-doped regions (DMS-like) in the vicinity of the Mn δ layers and unintentionally Mn-doped GaAs interlayer regions (dopedlike). The cross-sectional scanning tunneling microscopy (X-STM) studies of Yakunin[12] on these samples have demonstrated that Mn is well confined near the δ layer, i.e., 80% of Mn is located in the first monolayer (lattice plane) and only 20% in the next left and right neighboring monolayers. However, we expect the presence of Mn at the background level in the undoped GaAs interlayer regions. The resulting HPL spectrum from the DFHs is thus a superposition of DMS-like and dopedlike spectra. As the number of the Mn δ layers in all DFH structures is fixed, we can expect the HPL intensity from the DMS-like regions to be about the same for all samples and independent of the interlayer distance. On the other hand, the HPL intensity from the unintentionally doped regions should increase with interlayer distance due to the increase in the volume contributing to the HPL. However, in contrast to this expectation, the DMS-like HPL spectrum actually becomes weaker with interlayer distance and, moreover, transforms to the dopedlike HPL spectrum.

This behavior of the HPL spectra can be understood by the assumption that holes in the impurity band of the DMS layers become more and more compensated by electrons supplied from the GaAs interlayers. These electrons originate from As antisites (double donors), which were also observed in the X-STM studies of Yakunin[12] and from interstitial Mn (double donors).[11,13] This compensation also leads to the observed redshift of the HPL high-energy cutoff (marked by arrows with the label "0" in Fig. 1). The high-energy cutoff of the HPL spectrum from each sample corresponds to the recombination of electrons from the point of creation with holes bound to single Mn acceptors.[10,11,14] The energy shift (δE) of the HPL spectrum cutoff 0 with respect to the exciting laser line in the Mn-doped GaAs sample (D^{LT}) depends on the binding energy of the Mn acceptor (E_{Mn}) and the kinetic energy of heavy holes (ε_{hh}) in the point of creation $\delta E = \varepsilon_{hh} + E_{Mn}$ [see Fig. 2(a)]. In the (Ga,Mn)As DMS sample, this δE is smaller than in the Mn-doped GaAs sample because of the impurity-band formation. One can see with the help of the scheme on the left side of Fig. 2(a) that impurity band formation reveals itself in the blue shift (i.e., δE decrease) of high-energy HPL cutoff 0 because electrons from the point of creation can recombine with holes occupying impurity band states with an energy lower than the binding energy of the isolated Mn acceptor. However, in the donor-compensated DMS, the holes predominantly populate the upper states of the impurity band due to compensation of the holes occupying the lower states. Therefore, δE effectively increases and the resulting HPL exhibits the observed redshift of its cutoff "0."

Figure 3(b) shows the magnetic field dependence of the

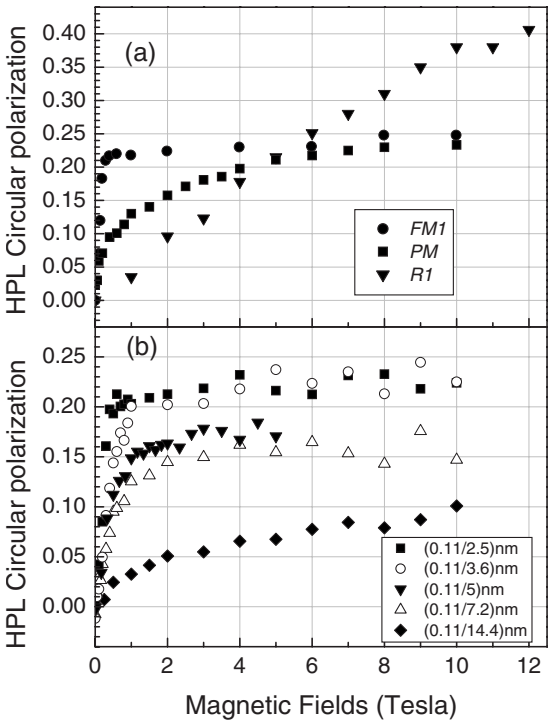

FIG. 3. Magnetic field dependence of the HPL circular polarization measured at 5 K in Faraday geometry (a) for bulk (FM1) and (PM) DMSs and bulk GaAs:Mn (R1) (b) for different DFHs.

HPL circular polarization measured at its onset 0 for the DFH samples with different GaAs interlayer thicknesses. For comparison, we present in Fig. 3(a) the data obtained from bulk ferromagnetic (FM1) and paramagnetic (PM) (Ga,Mn)As samples, as well as the Mn-doped GaAs sample R1. The increase in the GaAs interlayer thickness manifests itself in two aspects. First, the slope (i.e., polarization rate $[(d\rho(B)/dB)_T]$) of the polarization curves measured in the low magnetic field limit ($B \leq 1$ T) decreases with the GaAs interlayer thickness. Second, the HPL polarization measured at the saturating magnetic field significantly decreases when the distance between the FM sheets exceeds 5 nm. A comparison of the polarization curves of DFH samples to those of the FM and PM reference samples shows that they exhibit a rather FM-like behavior. Only the DFH sample with the largest interlayer separation exhibits a borderlike FM-PM behavior. The decrease in the polarization rate, which is proportional to the spontaneous magnetization M_s $[(d\rho(B)/dB)_T \propto M_s(T)^2/T]$,[10,11] means that the ferromagnetic properties of the δ layers relax as the interlayer distance d increases. This magnetization behavior is supported by the results of SQUID measurements.

Let us now discuss the effect of interlayer separation on the HPL polarization at the saturating magnetic field. In Refs. 10, 11, and 15, it was demonstrated that the maximum value of the HPL polarization strongly depends on the value and the sign of the random fields acting on single Mn acceptors or on the impurity band. For a local tensile stress field, the HPL polarization tends to the value $\rho_c(B \to \infty) = 0.27$ while for a compressive stress field the polarization is $\rho_c(B) = 0$. A careful analysis of our data demonstrates that the increase in

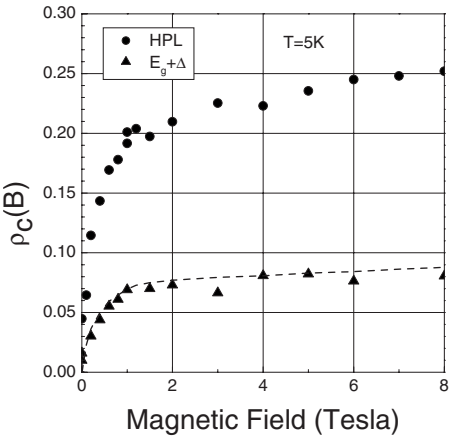

FIG. 4. Magnetic field dependence of the PL circular polarization measured at 5 K in spectral points 0 and $E_g+\Delta$ in Faraday geometry for DFH (0.11/5). The dashed line represents the rescaled dependence of the HPL circular polarization on a magnetic field.

the distance d between the DMS δ layers reduces the ferromagnetism in the DFH structures in two ways. First of all, electrons coming from the interlayer regions effectively compensate for the impurity band holes participating in the ferromagnetic ordering. On the other hand, thicker interlayer regions induce stress in the DMS δ sheets. Due to this stress, the ground state of the impurity band becomes unpolarized.

We already noted that the unintentionally Mn-doped GaAs interlayer regions can contribute to the HPL spectra. This is seen in Fig. 1(a) in the broad PL peak located at $\approx$1.86 eV, which arises from the recombination of free or donor-bound (Mn double donor) electrons with holes photogenerated in the spin-orbit split-off subband ($E_g+\Delta$ line) [see the scheme of optical transitions in Fig. 2(b)]. This line was detected in Mn-doped bulk GaAs and assigned to recombination of free (photoexcited) or Mn double donor bound electrons with holes photoexcited in the $E_g+\Delta$ valence subband.[11] We believe that the electrons located in the GaAs interlayer regions are responsible for this line. Indeed, in the FM δ sheets the Mn double donors are mostly ionized due to the compensation of holes bound to the impurity band. In contrast, the GaAs interlayer regions are Mn doped at the background level and therefore, the capture of photocreated electrons on Mn double donor states with their following recombination with holes from the spin-orbit split-off subband (sh) is more probable.

The observation of the $E_g+\Delta$ line in the HPL spectra opens a unique possibility to study the electron polarization[16] in the interlayer regions of Mn/GaAs DFH structures. Figure 4 shows the magnetic field dependence of the PL circular (see filled triangles) polarization measured in the maximum of the ($E_g+\Delta$) line. The measured circular polarization of this line in a magnetic field is directly related to the spin polarization of electrons. Indeed, the holes excited in the spin-orbit split-off subband rapidly relax to the light and heavy hole subbands. The typical energy relaxation time ($\sim 10^{-13}$ s) (Ref. 17) of holes in this subband is much shorter than any possible spin relaxation time. The spins of sh holes recombining with equilibrium free or Mn donor bound electrons are therefore not oriented by the external magnetic field and do not contribute to the circular polarization of the $E_g+\Delta$ line. The magnetic field induced circular polarization of the $E_g+\Delta$ line is thus exclusively related to the magnetization of electrons. The maximum theoretical value for the polarization of the $E_g+\Delta$ line is equal to $\rho_0=1$. However, for finite spin relaxation (τ_s) and life (τ_0) times of electrons, this maximum polarization can be significantly reduced to $\rho=(1+\tau_s/\tau_0)^{-1}\rho_0$. A comparison of the PL polarization data measured from the DMS δ layers (filled circles) and those from the GaAs interlayers (filled triangles in Fig. 4) shows that they demonstrate similar behavior on a magnetic field. Indeed, the rescaled HPL polarization curve (shown by the dashed line in Fig. 4) coincides very well with the measured data in the maximum of the $E_g+\Delta$ line. This means that the spin polarization of the holes in the DMS δ layers and electrons in the GaAs interlayers is proportional to the magnetization of the FM δ sheets. We conjecture that the strong spin polarization of electrons in the GaAs interlayers is related to an exchange interaction with FM δ sheets rather than to a much weaker dipolar magnetic field from these sheets. On the other hand, it is obvious that the exchange field is smaller for electrons than for holes due to a smaller wave function overlap with Mn δ sheets as well as a smaller constant of s-d exchange [$\alpha N_0=0.17$ eV (Ref. 18)] in comparison to the constant of p-d exchange [$\beta N_0=-1.2$ (Ref. 19)].

B. Hot electron photoluminescence polarization in granular diluted magnetic semiconductors

Next, we examine the other possibility to polarize the carriers in the GaAs matrix now containing ferromagnetic metallic MnAs nanocrystals. In Refs. 8 and 9, Moreno *et al.* demonstrated that such systems can be obtained by rapid thermal annealing of ferromagnetic ternary (Ga,Mn)As alloys. Figure 5 shows the HPL spectra obtained from the as-grown sample FM2 (spectrum 1) and after rapid thermal annealing from $FM2^{RTA}$ (spectrum 2). Sample FM2 shows a very weak HPL and the absence of any band-gap PL related to the $e \rightarrow A^0$ transition. After rapid thermal annealing, the HPL signal becomes more intense. Note that RTA totally suppresses the band gap PL originating from the substrates. This effect can be explained by the high density of metallic MnAs clusters generated by RTA.[8] Such clusters effectively screen the substrates from excitation laser. The annealing also strongly modifies the magnetic field dependence of the circular polarization of the HPL. The data in Fig. 6 show the magnetic field dependencies of the circular polarization from sample FM2 (solid circles) and from sample $FM2^{RTA}$ (open circles) obtained at $T=5$ K. In sample FM2, the polarization rate in low magnetic fields and its saturating value are very similar to those observed in all ternary (Ga,Mn)As DMS samples. In contrast, the hole polarization in sample $FM2^{RTA}$ follows pretty well that observed in the reference samples (R1), i.e., it shows paramagnetic-type behavior, and the saturating polarization is between that of the as-grown FM2 and reference (R1) samples. Thus, one can clearly see that rapid thermal annealing destroys the ferromagnetic ordering that exists in ternary (Ga,Mn)As DMS. On the other hand, the

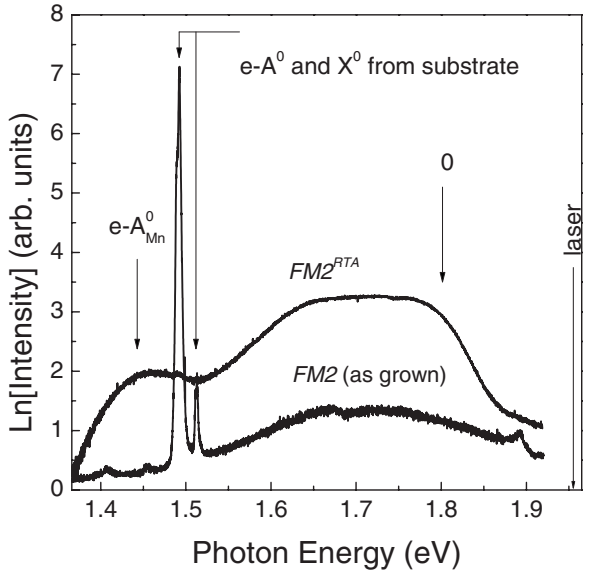

FIG. 5. HPL spectra of (FM2) DMS samples as grown and (FM2^{RTA}) RTA excited with a He-Ne laser (1.96 eV) at $T=5$ K. The arrows labeled 0 indicate the energy for recombination of electrons from the point of generation. The recombination of thermalized electrons with holes bound to Mn acceptors in (FM2^{RTA}) sample is marked by $e-A^0_{Mn}$.

annealing partially removes the random local stress or electric fields in the GaAs matrix. It was demonstrated in Refs. 8 and 9 that upon annealing, a phase separation occurs, the Mn and the excess As leave the zincblende matrix to form (Mn,Ga)As clusters (nanocrystals), and the compressive strain disappears. These nanocrystals were found to have bimodal size distribution, small size around 10 nm and the larger cluster around 50 nm, while the average intergranular distance was about 50 nm.

The phase separation that occurs during RTA of ternary (Ga,Mn)As alloys can explain the observed effect of annealing on the hole polarization. The formation of MnAs significantly reduces the average density of Mn acceptors in the GaAs matrix. This leads to the breakdown of the Mn impurity band and to the appearance of isolated Mn acceptors.

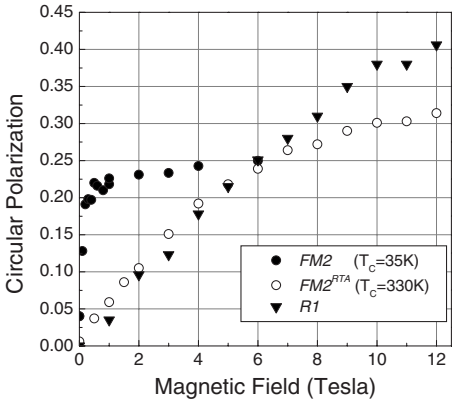

FIG. 6. Magnetic field dependence of the HPL circular polarization measured at 5 K in Faraday geometry for as-grown (FM2), RTA DMS (FM2^{RTA}), and reference doped R1 samples.

The phase separation also leads to the relaxation of stress in the matrix of the RTA-treated samples. Therefore, the polarization of holes bound to isolated Mn acceptors show a magnetic field dependence of the polarization similar to that observed in the Mn-doped GaAs reference sample. The important result of the study of the annealing effect on the hole polarization is that despite the (macroscopic) ferromagnetic behavior of the RTA-treated sample up to room temperatures, as measured by SQUID, the polarization of holes in the GaAs matrix follows the paramagnetic-type behavior. This means that there is no significant diffusion of magnetization from the ferromagnetic MnAs nanocrystals into the GaAs matrix in GaAs:MnAs granular materials. This effect can be explained by a model assuming that each metallic MnAs nanocrystal is surrounded by a noticeable depletion sphere $L\sim\sqrt{U_s/N_{Mn}}$ (where U_s is a metal-semiconductor junction potential and N_{Mn} is the Mn concentration in the GaAs matrix). This relatively large depletion sphere ($L\sim 30$ nm for Mn concentration in the matrix $N_{Mn}\sim 10^{18}$ cm^{-3}) prevents the penetration of the wave function of acceptor or impurity bound holes to the MnAs nanocrystals. Therefore, one can exclude the polarization of the holes due to exchange interaction (in contrast to DFHs) with MnAs nanocrystals. On the other hand, Mn acceptors located outside of the depletion sphere experience a dipolar magnetic field induced by single domain, which is however weaker than the external magnetic field. The comparison of the magnetic field induced spin polarization of carriers in DFHs and granular DMS material shows that the latter is less appropriate as a source of spin polarized carriers.

IV. CONCLUSION

The carrier polarization in ferromagnetic Mn/GaAs DFHs and granular GaAs:MnAs has been studied by hot-electron photoluminescence. We found that the increase in the distance between the ferromagnetic Mn δ layers leads to the relaxation of the ferromagnetic properties of DFHs and a decrease in the carrier polarization. This effect is caused by hole compensation in the DMS regions by electrons originating from the GaAs interlayers. The other important factor is the stress imposed on the DMS regions from the thicker GaAs interlayers. Due to this stress, the spin unpolarized state of the impurity band becomes the ground state. Another important result of our investigations is that the holes in the ferromagnetic DMS regions as well as the electrons in the GaAs interlayers experience a magnetic field proportional to the DMS δ layers magnetization. This opens the possibility to manipulate the electron spin state in the GaAs interlayers by varying the magnetic state of the ferromagnetic δ layers.

We have finally shown that rapid thermal annealing strongly modifies the ferromagnetic properties of ternary (Ga,Mn)As alloys. Nominally ferromagnetic (Ga,Mn)As DMS phase-separate into ferromagnetic MnAs nanocrystals and a paramagnetic GaAs matrix after RTA. Contrary to the DFH structures, the carriers in the GaAs matrix do not feel the strong magnetic field of the MnAs nanocrystals despite the measured macroscopic Curie temperature of 330 K for the granular GaAs:MnAs material.

ACKNOWLEDGMENTS

We thank X. X. Guo, C. Herrmann, D. Kolovos-Vellianitis, and M. Moreno for the growth of the samples under investigation; N. S. Averkiev, O. Brandt, I. E. Panaiotti, and M. Ramsteiner for helpful discussions; G. Paris for invaluable technical assistance; and L. Däweritz for continuous support and encouragement. Furthermore, we are indebted to L. Schrottke for critically reading the paper. One of us (V.F.S.) acknowledges the financial support from the Paul-Drude-Institute, the Russian Foundation for Basic Research (Grant No. 06-02-16245), Scientific Program of RAS, and SRDF RUP (Grant No. 1-2890-ST-07).

*sapega@dnm.ioffe.rssi.ru

[1] H. Ohno, A. Shen, F. Matsukura, A. Oiwa, A. Endo, S. Katsumoto, and Y. Iey, Appl. Phys. Lett. **69**, 363 (1996).
[2] K. W. Edmonds, P. Boguslawski, K. Y. Wang, R. P. Campion, S. N. Novikov, N. R. S. Farley, B. L. Gallagher, C. T. Foxon, M. Sawicki, T. Dietl, M. Buongiorno Nardelli, and J. Bernholc, Phys. Rev. Lett. **92**, 037201 (2004).
[3] R. K. Kawakami, E. Johnston-Halperin, L. F. Chen, M. Hanson, N. GueŽbels, J. S. Speck, A. C. Gossard, and D. D. Awschalom, Appl. Phys. Lett. **77**, 2379 (2000).
[4] X. X. Guo, C. Herrmann, X. Kong, D. Kolovos-Vellianitis, L. Däweritz, and K. H. Ploog, J. Cryst. Growth **278**, 655 (2005).
[5] X. Kong, A. Trampert, X. X. Guo, L. Däweritz, and K. H. Ploog, J. Appl. Phys. **97**, 036105 (2005).
[6] X. Kong, A. Trampert, X. X. Guo, D. Kolovos-Vellianitis, L. Däweritz, and K. H. Ploog, J. Appl. Phys. **97**, 094913 (2005).
[7] Y. L. Soo, S. Wang, S. Kim, G. Kim, M. Cheon, X. Chen, H. Luo, Y. H. Kao, Y. Sasaki, X. Liu, and J. K. Furdyna, Appl. Phys. Lett. **83**, 2354 (2003).
[8] M. Moreno, A. Trampert, B. Jenichen, L. Däweritz, and K. H. Ploog, J. Appl. Phys. **92**, 4672 (2002).
[9] M. Moreno, V. M. Kaganer, B. Jenichen, A. Trampert, L. Däweritz, and K. H. Ploog, Phys. Rev. B **72**, 115206 (2005).
[10] V. F. Sapega, M. Moreno, M. Ramsteiner, L. Däweritz, and K. Ploog, Phys. Rev. Lett. **94**, 137401 (2005).
[11] V. F. Sapega, M. Ramsteiner, O. Brandt, L. Däweritz, and K. H. Ploog, Phys. Rev. B **73**, 235208 (2006).
[12] A. M. Yakunin, Ph.D. thesis, Eindhoven University of Technology, 2005.
[13] K. M. Yu, W. Walukiewicz, T. Wojtowicz, I. Kuryliszyn, X. Liu, Y. Sasaki, and J. K. Furdyna, Phys. Rev. B **65**, 201303(R) (2002).
[14] I. Ya. Karlik, I. A. Merkulov, D. N. Mirlin, L. P. Nikitin, V. I. Perel', and V. F. Sapega, Fiz. Tverd. Tela (Leningrad) **24**, 3550 (1982) [Sov. Phys. Solid State **24**, 2022 (1982)].
[15] N. S. Averkiev, A. A. Gutkin, E. B. Osipov, and M. A. Reshchikov, Fiz. Tverd. Tela (Leningrad) **30**, 765 (1988) [Sov. Phys. Solid State **30**, 438 (1988)].
[16] D. N. Mirlin, L. P. Nikitin, and V. F. Sapega, Fiz. Tekh. Poluprovodn. (S.-Peterburg) **28**, 3650 (1986) [Sov. Phys. Semicond. **28**, 3731 (1986)].
[17] A. G. Aronov, D. N. Mirlin, L. P. Nikitin, I. I. Reshina, and V. F. Sapega, Pis'ma Zh. Eksp. Teor. Fiz. **29**, 69 (1979) [JETP Lett. **29**, 60 (1979)].
[18] V. F. Sapega, T. Ruf, and M. Cardona, Phys. Status Solidi B **226**, 339 (2001).
[19] J. Okabayashi, A. Kimura, O. Rader, T. Mizokawa, A. Fujimori, T. Hayashi, and M. Tanaka, Phys. Rev. B **58**, R4211 (1998).